

# Selective Production of Hydrogen by Partial Oxidation of Methanol over ZnO-Supported Palladium Catalysts

M. L. Cubeiro\* and J. L. G. Fierro†<sup>1</sup>

\* Centro de Catálisis, Petróleo y Petroquímica, Escuela de Química, Facultad de Ciencias, Universidad Central de Venezuela, A.P. 47102, Los Chaguaramos, Caracas, Venezuela; and † Instituto de Catálisis y Petroquímica, CSIC, Campus UAM, Cantoblanco, 28049 Madrid, Spain

Received September 9, 1997; revised October 24, 1997; accepted October 29, 1997

Hydrogen production by partial oxidation of methanol ( $\text{CH}_3\text{OH} + 1/2 \text{O}_2 \rightleftharpoons 2 \text{H}_2 + \text{CO}_2$ ) was studied over zinc oxide-supported Pd catalysts. Catalyst performance was investigated as a function of the Pd loading and pretreatment in hydrogen environment under feed ratios  $\text{O}_2/\text{CH}_3\text{OH}$  (molar) of 0.3 and 0.5 at 503–543 K. High yields of hydrogen were obtained under integral operation regime. The hydrogen selectivity showed a strong dependence on the methanol conversion, which suggests that oxidation and reforming steps take place consecutively. Catalyst characterization by temperature-programmed reduction, X-ray diffraction, and X-ray photoelectron spectroscopy revealed that PdZn alloys can be formed upon reduction at moderate temperatures. A shift of +0.7 eV has been observed in the binding energy of Pd  $3d_{5/2}$  core level spectrum of catalyst 1% Pd/ZnO prerduced at temperatures as low as 373 K and catalyst 5% Pd/ZnO reduced at 573 K and above. The relative ease with which PdZn alloy is formed in 1% Pd/ZnO catalyst is explained in terms of a stronger metal–metal oxide interactions of the smaller Pd particles. PdZn alloys were also detected by X-ray diffraction on the 2% Pd/ZnO catalyst after on-stream operation. Pretreatments of the catalysts in hydrogen at high temperatures led to sintering of metallic particles with the subsequent drop in methanol conversion. © 1998 Academic Press

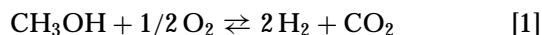
## INTRODUCTION

The scarcity of fossil fuels and the associated pollutions problems during their combustion have attracted the attention towards the search of alternative fuels (1–3). Hydrogen gas, whether used directly as a fuel in internal combustion engines (2,4) or indirectly to supply electricity using fuel cells (5,6), is inherently clean burning and highly reactive so that high thermal efficiencies can be obtained. When used in internal combustion engines the compression ratio can be increased markedly and because of its wide combustion limits hydrogen can be burnt in mixtures much leaner than is possible using conventional hydrocarbon/air mixtures. Thermal efficiencies in the order 35–40% may thus

be achieved, in comparison with the 25–30% typical of a normal petrol fuelled engine (7).

The second option are fuel cells. Fuel cells are attractive in terms of potentially high energy conversion efficiencies, and for these hydrogen is orders of magnitude more reactive than any other fuel (8). The major impediment to the wider use of hydrogen as an energy source are the difficulties inherent in storage, distribution and transportation. One solution to the storage problem is the on-board hydrogen generation from a suitable high energy density fuel such as methanol. Hydrogen can be obtained directly from methanol according to three different processes: partial oxidation, thermal decomposition (4,9) and steam reforming. When used in engine and vehicle technologies, methanol partial oxidation offers some advantages in respect to methanol steam reforming (1,6) as it requires oxygen (air) instead water, and it is an exothermic reaction which does not require heat supply.

Partial oxidation of methanol with oxygen or air (reaction [1]) and steam reforming (reaction [2]), under specific reaction conditions produces almost quantitatively  $\text{H}_2$  and  $\text{CO}_2$ :



While reaction [1] is exothermic, reaction [2] is endothermic and produces more favourable  $\text{H}_2/\text{CO}_2$  ratios. Cu–ZnO based methanol synthesis catalysts have been extensively studied in the steam reforming (5,6,10,11) and to lesser extent in the partial oxidation reaction (6,12–14). Considering the different processes involved in the partial oxidation, two options have been considered: (i), combination of combustion-reforming through consecutive beds of noble metal and copper catalyst, respectively (10); and (ii), oxygen incorporation during steam reforming over copper catalysts (12,13).

Group VIII noble metals such as palladium and platinum have been found active in methanol transformation although they are less selective in the steam reforming,

<sup>1</sup> To whom correspondence should be addressed.

yielding primarily the decomposition products CO and H<sub>2</sub>. Apart from this general trend, the behaviour of Pd-ZnO catalyst seems to be close to that of the conventional Cu-ZnO methanol synthesis ones. In this respect, Takezawa *et al.* (15,16) reported exceptional performance of Pd-ZnO catalysts, not only in the steam reforming, but also in the dehydrogenation of methanol to methyl formate, reactions otherwise conducted with high selectivities over copper catalysts. These authors attributed this particular behaviour of Pd-ZnO systems to the formation of PdZn alloys at the metal-support interface.

These peculiar characteristics of Pd-based catalysts mentioned above, together with our experience on Cu-ZnO systems (1,14,17,18), prompted us to study the effect of Pd loading and reaction conditions on the performance of Pd-ZnO for the partial oxidation of methanol. Therefore, we prepared ZnO-supported Pd catalysts with Pd loadings ranging from 1 to 5% and then tested in the partial oxidation of methanol at atmospheric pressure. Parallel characterization of catalyst structures have already been performed with X-ray diffraction, temperature-programmed reduction and photoelectron spectroscopy.

## EXPERIMENTAL

### Catalyst Preparation

The ZnO carrier was prepared by thermal decomposition of Zn oxalate. Zinc oxalate was prepared by precipitation of a Zn(NO<sub>3</sub>)<sub>2</sub> · 6H<sub>2</sub>O (Aldrich, purity >98%) solution by dropwise adding at 313 K of another H<sub>2</sub>C<sub>2</sub>O<sub>4</sub> · 2H<sub>2</sub>O (Pan-reac, pa) solution (16.5% in excess). The initial concentrations of zinc nitrate and oxalic acid were 18.7 and 1.8 M, respectively. After complete precipitation, the excess water was removed under vacuum at 353 K. Thermal decomposition of ZnC<sub>2</sub>O<sub>4</sub> was performed in air in two steps: 418 K for 0.5 h; then the temperature was increased at a rate of 5 K/min up to 653 K and maintaining this temperature for 0.5 h. Since the product exhibited a grey colour, probably because of ZnO defect structure, the oxide was subsequently calcined in air at 673 K for 4 h while its colour turned white.

Four Pd-ZnO catalysts were prepared by impregnation of ZnO (particle size 70 nm) with aqueous solutions of Pd(NO<sub>3</sub>)<sub>2</sub> · 2H<sub>2</sub>O (Fluka, purum >98%). Two catalysts, nominal Pd contents of 1 and 2%, were prepared by the incipient wetness impregnation method using a solution/solid ratio = 1 (ml/g), and two other catalysts, nominal Pd content 1 and 5%, by the impregnation in excess of solution (10 and 7 ml solution/g ZnO, respectively). After contacting ZnO with the Pd solution at pH close to 3, a brown precipitate was formed. Although this precipitate was solubilized by dropwise adding dilute nitric acid, it persists at the end of the impregnation. The impregnates were dried at 383 K for 8 h and then calcined in air at 623 K for 3 h.

### Experimental Techniques

The palladium content of the catalysts was determined by atomic absorption spectrometry using a Perkin Elmer 3030 instrument. The solids were kept in contact with a HCl + HNO<sub>3</sub> mixture in a hermetical container and digested in a microwave oven over 1 h.

Powder X-ray diffraction (XRD) patterns of the samples were recorded on a Seifert 3000P diffractometer with a nickel-filtered CuKα<sub>1</sub> (λ = 0.15406 nm) radiation scanning 2θ angles ranging from 5 to 75°. Thermogravimetric analysis of the Zn-oxalate precursor was performed with a Perkin Elmer TGA 7 instrument working at a heating rate of 5 K/min and under air flow (60 ml/min). Specific areas of the catalysts were calculated by applying the BET method to the nitrogen adsorption isotherms obtained at liquid nitrogen temperature on outgassed samples at 413 K using an automatic ASAP 2000 adsorption instrument. Temperature-programmed reduction (TPR) experiments were carried out in a semiautomatic Micromeritics TPD/TPR 2900 apparatus interfaced to a microcomputer. TPR profiles were obtained by passing a 10% H<sub>2</sub>/Ar flow (50 ml/min) through the sample (about 70 mg). The temperature was increased from 305 to 1000 K at a rate of 10 K/min, and the amount of H<sub>2</sub> consumed was determined with a thermoconductivity detector (TCD); the effluent gas was passed through a cold trap placed before the TCD in order to remove water from the exit stream.

Photoelectron spectra (XPS) were acquired with a VG ESCALAB 200R spectrometer equipped with a hemispherical electron analyzer and Mg Kα (hν = 1253.6 eV, 1 eV = 1.6302 × 10<sup>-19</sup> J) 120-W X-ray source. The powder samples were evacuated in the pretreatment chamber of the instrument at 295 and 573 K for 2 h and reduced in H<sub>2</sub> at temperatures ranging from 305 to 773 K for 2 h. The residual pressure in the ion-pumped analysis chamber was maintained below 5 × 10<sup>-9</sup> Torr during data acquisition. The intensities of Zn 2p<sub>3/2</sub> and Pd 3d<sub>5/2</sub> peaks were estimated by calculating the integral of each peak after smoothing and subtraction of the "S-shaped" background and fitting the experimental curve to a combination of Gaussian and Lorentzian lines of variable proportion. The binding energies (BE) were referenced to the C 1s peak at 284.9 eV, this reference giving BE values with an accuracy of ±0.1 eV.

### Activity Measurements

Catalytic experiments for methanol oxidation were performed at atmospheric pressure in a continuous flow system with a stainless steel tubular reactor 6.3 mm ID, using 0.2 and 0.5 g of catalyst (particle size 0.42-0.59 mm) held between quartz glass wool portions with a preheating section packed with SiC at the top and an Inconel filter at the bottom. The temperature of the reactor was maintained by an electronic controller which powers an electrical furnace

and uses a thermocouple as reference, placed 12 mm up the catalytic bed. The temperature at the catalyst bed was measured by a second thermocouple placed inside the catalyst bed. Methanol (Scharlau, HPLC grade) was fed by means of a liquid pump (Becton-Dickinson) at a rate of 2 ml/h and then vaporized in a preheater. The oxygen and nitrogen (diluent) flows were adjusted by mass flow controllers. The total flow was 100 ml(STP)/min, with a methanol molar concentration of 21.2% and O<sub>2</sub>/CH<sub>3</sub>OH ratios of 0.3 and 0.5. The samples were reduced *in situ* in a 10% H<sub>2</sub>/N<sub>2</sub> stream starting at room temperature for 0.5 h, then heating at a rate of 5 K/min up to 573 K and keeping this temperature for 0.5 h. Reaction temperatures explored covered the range 503–543 K. The analysis of the effluents of the reactor was performed with an on-line gas chromatograph (Varian 3400 CX) provided with a TC detector and two Porapack N and molecular 5A packed columns in series, using Ar as the carrier gas. Data over periods of 8–12 h on-stream were obtained for each set of fixed reaction conditions. The same sequence of variation on the O<sub>2</sub>/CH<sub>3</sub>OH ratio and the temperature for each catalyst sample was followed.

## RESULTS AND DISCUSSION

### Characterization of the Precursor

TGA and its derivative DTGA profiles of the Zn-oxalate carrier precursor are shown in Fig. 1. Two major decomposition peaks centred at 418 and 652 K can be observed. The weight loss of the former peak, which amounts 18.7%, fits well with the 19.0% expected for water removal from the Zn-oxalate hydrate [Zn(C<sub>2</sub>O<sub>4</sub> · 2H<sub>2</sub>O)], while the 37.9% weight loss of the latter closely corresponds to the theoretical one expected for the decomposition of Zn(C<sub>2</sub>O<sub>4</sub>)

into ZnO. These TGA and DTGA profiles clearly indicate that a minimum decomposition temperature of 673 K is required to obtain ZnO. As the BET area is expected to decrease with increasing decomposition temperature, the ZnO support was prepared by thermal decomposition of the Zn-oxalate hydrate precursor at 673 K.

The impregnation of the resulting ZnO with an aqueous solution of Pd nitrate appear quite complex due to the tendency of Pd(NO<sub>3</sub>)<sub>2</sub> to be hydrolyzed and also the ability of ZnO to be solubilized in acid solution (19). The Pd(NO<sub>3</sub>)<sub>2</sub> undergoes hydrolysis with the subsequent increase of the acidity of the solution (Pd(NO<sub>3</sub>)<sub>2</sub> + H<sub>2</sub>O ⇌ Pd(OH)(NO<sub>3</sub>) + NO<sub>3</sub><sup>-</sup> + H<sup>+</sup>). As the solubility of the Pd hydroxinitrate is very low, some precipitation is expected to occur. In our case, the extent of this process may be even larger because some solubilization of ZnO takes place upon contacting the support and the impregnant solution with the subsequent pH increase.

### Chemical Composition and Textural Properties

Chemical analyses by atomic absorption spectroscopy revealed that Pd content is close to the nominal one (Table 1). The shape of the N<sub>2</sub> adsorption isotherms and BET areas were conclusive that no microporosity developed. The BET area of the catalysts prepared according to the wetness impregnation method (1% Pd/ZnO and 2% Pd/ZnO) is similar to that of the starting ZnO carrier (Table 1). However, the BET area decreased drastically in the catalysts prepared by impregnation in excess solution (1% Pd/ZnO (ES) and 5% Pd/ZnO). This result suggests, as already advanced above, that a small fraction of ZnO is solubilized in acid medium during impregnation and again precipitated over the ZnO substrate at the end of impregnation when

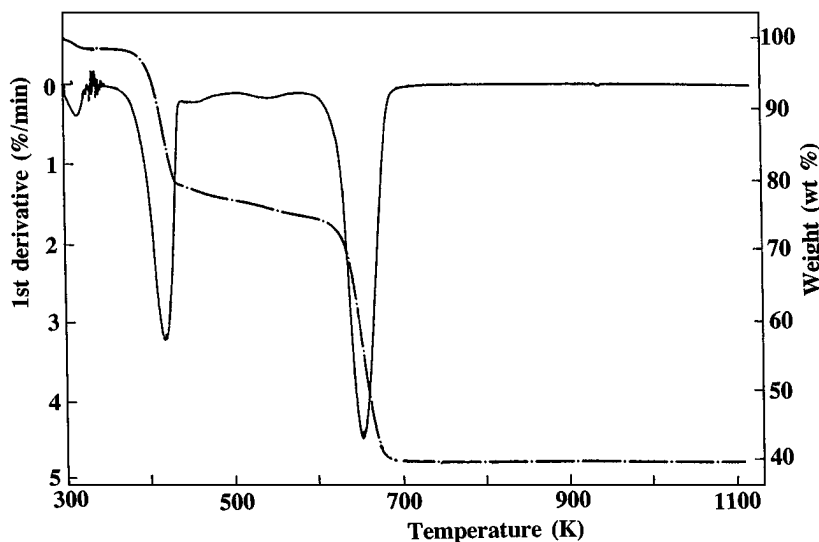


FIG. 1. Thermogravimetric (TG) and first derivative (DTG) curves of the zinc oxalate precursor under air flow (60 cm<sup>3</sup>/min) at a heating rate of 5 K/min.

TABLE 1

Chemical Composition and BET Area of Calcined Samples

Sample	Pd (wt%)	ZnO (wt%)	$S_{\text{BET}}$ (m <sup>2</sup> /g)
ZnO	—	—	10
1% Pd/ZnO (IW)	1.13	83.8	11
2% Pd/ZnO (IW)	2.43	89.9	9
1% Pd/ZnO (ES)	1.24	83.8	4
5% Pd/ZnO (ES)	5.20	84.8	4

Note. IW = incipient wetness; ES = excess of solution.

the water excess is completely removed. As the precipitated phase, presumably constituted by  $\text{Zn}(\text{NO}_3)_2$ , can be accommodated within the macropores of the original ZnO carrier, a fraction of the pores of the original ZnO sample can be blocked by this solubilized and precipitated ZnO phase.

### X-Ray Diffraction (XRD)

XRD patterns of ZnO carrier and 1% Pd/ZnO catalysts exhibited diffraction lines of ZnO phase but in no case that of Pd metal or its compounds. Considering the low Pd loading, the absence of diffraction lines of PdO may be due to its high dispersion degree on the ZnO surface. It is also emphasized in this point that the most intense diffraction line of PdO (PdO(101)) is positioned at a Bragg's angle of  $33.9^\circ$  which would be overshadowed by the strong ZnO(002) reflection at a Bragg's angle of  $34.4^\circ$ . However, as the other less intense Pd reflections which do not overlap with any reflections from ZnO were absent, no bulk Pd is found by XRD. The XRD diffraction patterns of calcined Pd/ZnO catalysts with different Pd loadings are displayed in Fig. 2. The diffraction lines of catalysts 1% Pd/ZnO (ES) and 5% Pd/ZnO (ES) appeared substantially narrower than that of the ZnO carrier and their 1% Pd/ZnO (IW) and 2% Pd/ZnO counterparts, prepared by the incipient wetness method. This finding indicates that the crystal size of ZnO particles is larger in the samples prepared in excess of solution, which agrees with their lower BET areas.

A complete study by XRD was carried out on the catalyst 2% Pd/ZnO (IW). Figure 3 includes the XRD patterns of this catalyst after hydrogen pretreatments and used in the methanol partial oxidation. The catalyst 2% Pd/ZnO (IW) calcined and reduced in hydrogen at 573 K (Figs. 3a and b, respectively) basically exhibit the pattern of ZnO. However, the pattern 3c of the catalyst reduced at 573 K and used in the reaction for 160 h on-stream at a maximum temperature of 563 K, and pattern 3d of the catalyst reduced at 623 K and then exposed to the reaction mixture for 90 h at temperatures ranging from 503 to 543 K display a broad and small peak at a Bragg's angle of  $41.2^\circ$ . A similar peak at the same position is clearly discerned in the catalyst 5% Pd/ZnO prerduced at 573 K (Fig. 3e). This peak cannot be indexed to either  $\text{Pd}^\circ$  or PdO because the Pd(111)

reflection of Pd metal would be positioned at  $40.1^\circ$  and the PdO(110) peak at  $41.9^\circ$ . In this latter case other more intense reflections of PdO would be observed. In the light of these observations and considering data from the literature (16,20–22), the peak at a Bragg's angle of  $41.2^\circ$  can be reasonably assigned to a PdZn alloy. The presence of this alloy in the catalyst during on-stream operation suggests that Pd when alloyed is resistant toward oxidation.

### Temperature-Programmed Reduction (TPR)

Since PdO is an easily reducible oxide, even at room temperature, the TPR experiments were carried out after sample conditioning and further exposure to the  $\text{H}_2/\text{Ar}$  mixture at room temperature. Hydrogen consumption was observed at room temperature in several experiments although its quantification became difficult, if not impossible, due to some fluctuations of the signal baseline just at the beginning of the experiment. The TPR profiles of ZnO-supported palladium catalysts are displayed in Fig. 4. Three regions can be distinguished: (i), the first one ranging from room temperature to 420 K; (ii), the second one in the 500–630 K range; and (iii) a steady increase above 670 K, with a clear peak at about 900 K in catalyst 5% Pd/ZnO. In general, it is apparent from Fig. 4 that the extent of  $\text{H}_2$ -consumption increased with increasing Pd loading. The

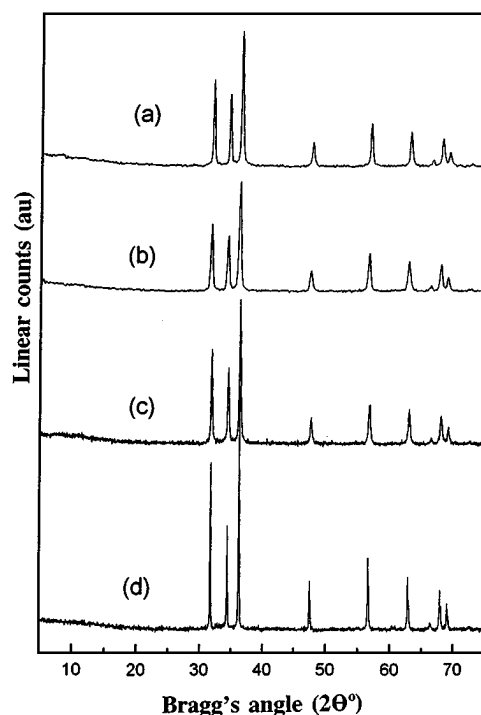


FIG. 2. XRD patterns of calcined Pd/ZnO catalysts with different Pd loadings: (b), 1% Pd/ZnO (IW); (c) 2% Pd/ZnO (IW); (d), 5% Pd/ZnO (ES). For comparative purpose the pattern of the ZnO carrier is also included (a).

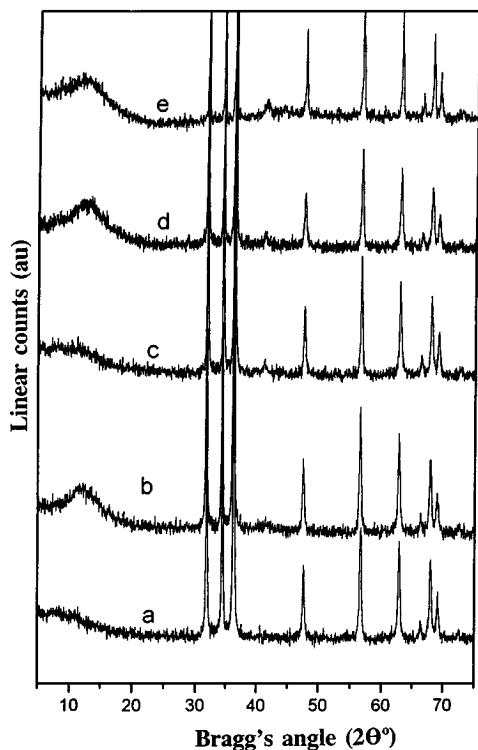


FIG. 3. XRD patterns of catalyst 2% Pd/ZnO subjected to various pretreatments: (a) calcined sample; (b) reduced in hydrogen at 573 K; (c) used catalyst reduced at 573 K; (d) used catalyst reduced at 623 K. For comparison, catalysts 5% Pd/ZnO reduced in hydrogen at 573 K is also included (e).

impregnation procedure does appear to have some influence on the redox properties of the catalysts. Thus the catalyst 1% Pd/ZnO (ES) was reduced at about 350 K, whereas its counterpart 1% Pd/ZnO (IW) was essentially reduced at ambient temperature (Figs. 4a and 4b). The interpretation of these profiles may be complicated not only by the observation of  $H_2$ -consumption peaks from both PdO and ZnO oxides but also by the formation of bulk palladium hydride. The first  $H_2$ -consumption peak at 300–420 K can be assigned to the reduction of PdO to Pd metal, whereas the broad peaks at 600 and 563 K observed for catalysts 1% Pd/ZnO (ES) and (IW) and at 617 and 553 K for 2% Pd/ZnO and 5% Pd/ZnO, respectively, may be associated to some reduction of ZnO substrate. As can be seen below in the XPS section, palladium became completely reduced at somewhat lower temperatures. Using Pd/ZnO catalysts, Hong *et al.* (20) found reduction of PdO, and also mildly of ZnO, to occur at room temperature, then Pd metal forms a hydride ( $H_xPd$ ) which decomposes at higher temperatures. Iwasa *et al.* (16) also observed that this hydride decomposes (negative peak in TPR profiles) at lower temperatures in ZnO-supported catalysts than in other carriers. Surprisingly, no hydride decomposition peak was observed in the Pd/ZnO catalysts reported in this study, which contrasts with Pd/AlO<sub>3</sub>, Pd/ZrO<sub>2</sub>, and Pd/SiO<sub>2</sub> systems (16,20).

As the Pd hydride is a bulk compound, the extent of hydride formation can be strongly affected by Pd dispersion. As confirmed by XPS measurements, the intensity of Pd 3d core level is rather high, even for the catalysts with 1% Pd loading, suggesting that metal is highly dispersed at the ZnO surface. Another alternate explanation is that a hydride can be decomposed once it is formed; therefore the negative peak of the hydride would be masked by the positive one due to the reduction of PdO. It is emphasized in this point that  $H_2$ -consumption at room temperature for the catalyst 1% Pd/ZnO (IW) was somewhat higher than the theoretical one expected for the quantitative reduction to Pd<sup>0</sup>, suggesting the formation of a certain proportion of Pd-like hydride species or even ZnO reduction. For catalyst 1% Pd/ZnO (ES) the first  $H_2$  consumption peak at 343 K was 1.7 times greater than the theoretical one for the PdO reduction. This result suggests that some reduction of the ZnO support can occur at low temperatures.

The progressive increase of TPR baseline for catalyst 2% Pd/ZnO at temperatures above 700 K and the observation of a broad and strong peak at ca 900 K for catalyst 5% Pd/ZnO indicate that another reduction process is involved in that temperature region. A blank TPR experiment using pure ZnO (not shown here) revealed the appearance of a broad feature somewhat above 800 K, as well as a sharp increase on the  $H_2$  consumption at ca 1000 K, indicative of the partial reduction of the ZnO substrate. In the light

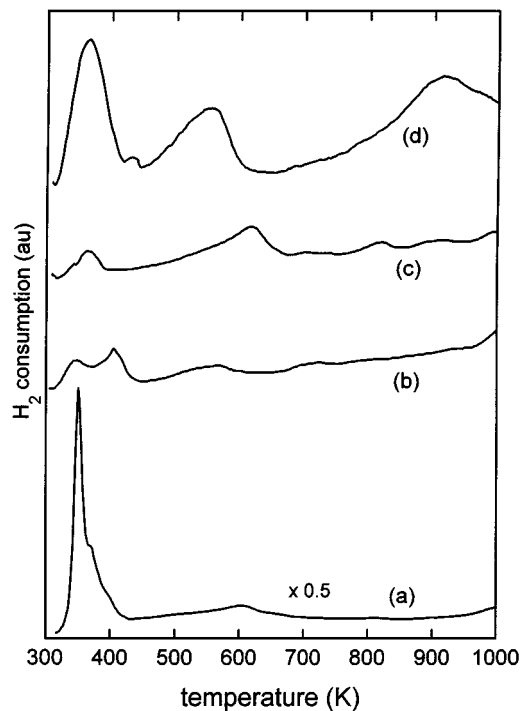


FIG. 4. TPR profiles of ZnO-supported palladium catalysts: (a) 1% Pd/ZnO (ES); (b) 1% Pd/ZnO (IW); (c) 2% Pd/ZnO (IW); and (d) 5% Pd/ZnO (ES).

TABLE 2

Binding Energies (eV) of Core Electrons and Surface (XPS) Atomic Ratios of Catalyst 1% Pd/ZnO Subjected to Different Pretreatments

Pretreatment	O 1s	Zn 2p <sub>3/2</sub>	Pd 3d <sub>3/2</sub>	Pd/Zn atom
Vacuum, RT	530.9(77)	1022.2	336.9	0.047
	532.4(23)			
Vacuum, 573 K	530.9(76)	1022.2	336.7(100)	0.045
	532.3(24)			
H <sub>2</sub> , RT	530.9(69)	1022.2	337.0(41)	0.036
	532.6(31)			
H <sub>2</sub> , 373 K	530.9(66)	1022.2	336.9(18)	0.034
	532.2(34)			
H <sub>2</sub> , 573 K	531.0(73)	1022.2	335.7(100)	0.033
	532.5(27)			
H <sub>2</sub> , 773 K	531.0(74)	1022.2	335.7(100)	0.031
	532.5(26)			

of this result, it is inferred that H<sub>2</sub>-consumption at high temperatures is associated to the reduction of bulk ZnO.

### Photoelectron Spectroscopy (XPS)

Photoelectron spectroscopy was used to study the chemical state of the elements and their relative abundance at catalyst surfaces. Two representative catalysts 1% Pd/ZnO (IW) and 5% Pd/ZnO (ES) were selected for this purpose, and the core level spectra recorded included O 1s, Zn 2p<sub>3/2</sub>, Pd 3d, and C 1s (as internal reference). The binding energies of core electrons and surface atomic ratios for catalysts 1% Pd/ZnO (IW) and 5% Pd/ZnO (ES) are summarized in Tables 2 and 3, respectively.

For the sake of clarity and in order to have an idea on peak profile, the Pd 3d core level of these two catalysts are displayed in Figs. 5 and 6, respectively. The profile of Pd 3d doublet was complex because of the overlapping Zn<sub>LMM</sub> Auger peak and the less intense Pd 3d<sub>3/2</sub> component. To

TABLE 3

Binding Energies (eV) of Core Electrons and Surface (XPS) Atomic Ratios of Catalyst 5% Pd/ZnO Subjected to Different Pretreatments

Pretreatment	O 1s	Zn 2p <sub>3/2</sub>	Pd 3d <sub>3/2</sub>	Pd/Zn atom
vacuum, RT	531.0(67)	1022.2	336.8(100)	0.182
	533.0(33)			
H <sub>2</sub> , RT	530.8(63)	1022.2	336.8(36)	0.494
	533.0(37)			
H <sub>2</sub> , 373 K	530.8(65)	1022.2	335.0(100)	0.333
	532.7(35)			
H <sub>2</sub> , 573 K	530.9(72)	1022.2	335.2(100)	0.242
	532.7(28)			
H <sub>2</sub> , 773 K	530.9(74)	1022.2	335.7(100)	0.207
	532.9(26)			

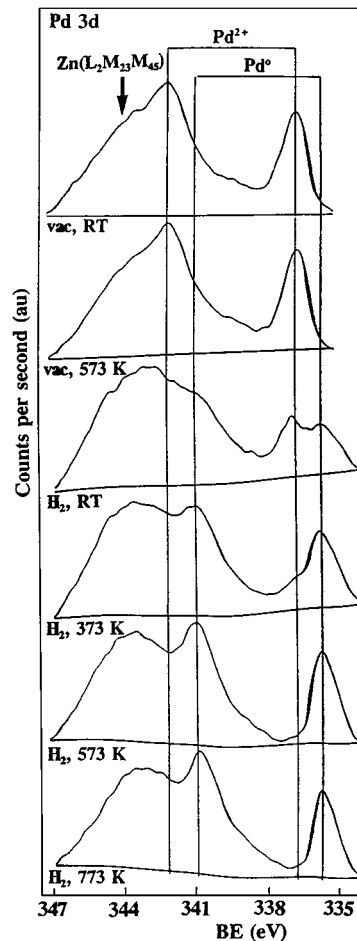


FIG. 5. Pd 3d core level spectra of catalyst 1% Pd/ZnO (IW) subjected to treatments of outgassing and H<sub>2</sub>-reduction at different temperatures.

avoid this difficulty, attention will be thereupon exclusively focused on the most intense Pd 3d<sub>5/2</sub> peak. Calcined samples exhibit a single Pd 3d<sub>5/2</sub> component with a BE of 336.8–336.9 eV (Figs. 5 and 6) which is typical of PdO species (16,23,24). Upon exposure to H<sub>2</sub> at room temperature, this oxide becomes reduced to a significant extent. By applying curve fitting procedures to the Pd 3d<sub>5/2</sub> envelope, a component at a BE of 335.5 eV, with a 59% of the whole area, for the sample 1% Pd/ZnO (IW) (Fig. 5), and at BE of 335.0 eV, with 65% of the area, for the sample 5% Pd/ZnO (ES) (Fig. 6) were observed. The extent of Pd reduction increased upon increasing the reduction temperature up to 373 K. Under these conditions, the area of the reduced Pd increased up to 82% for catalyst 1% Pd/ZnO (IW) (BE of Pd 3d<sub>5/2</sub> = 335.7 eV) (Fig. 5) and to 100% for catalyst 5% Pd/ZnO (ES) (Fig. 6). Reduction of catalysts at 573 and 773 K led to a single Pd 3d<sub>5/2</sub> component (Figs. 5 and 6). However, comparison of BEs of Pd 3d<sub>5/2</sub> peaks for samples reduced at higher temperatures reveals important differences. Thus, while catalyst 1 Pd/ZnO (IW) shows BEs at 335.7 eV when reduced at 373, 573, and 773 K, its 5%

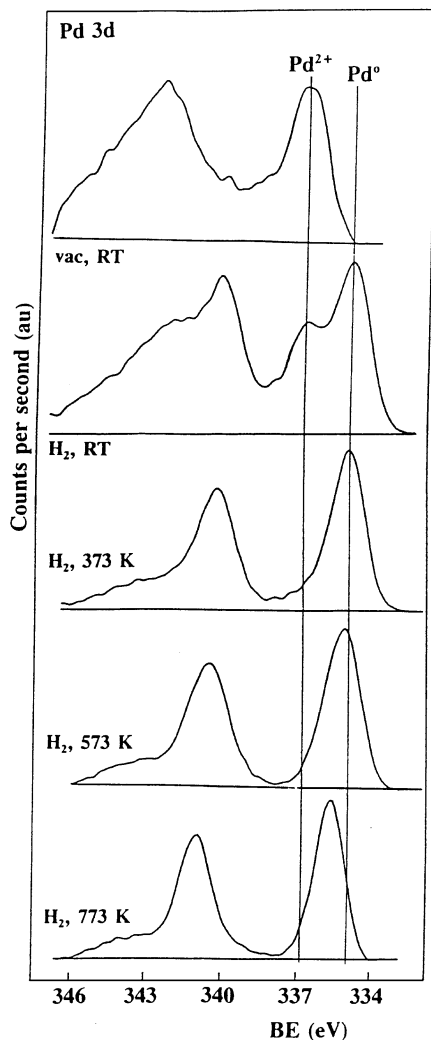


FIG. 6. Pd 3d core level spectra of catalyst 5% Pd/ZnO (ES) subjected to treatments of outgassing and H<sub>2</sub>-reduction at different temperatures.

Pd/ZnO (ES) counterpart displays BEs at 335.2 eV for the catalyst reduced at 573 K and increased up to 335.7 eV for the catalyst reduced at 773 K.

From an inspection of the BE values of Pd 3d<sub>5/2</sub> core level of several supported-palladium catalysts (16,23,25–27), it becomes apparent that BE close to 335 eV are responsible of Pd<sup>0</sup> species (16,23–29). Slightly higher BE values than this for the Pd 3d<sub>5/2</sub> core level have been reported for Pd supported in redox oxides (16) or for Pd-deposited on single crystals (26) and assigned to alloy formation (PdM<sub>x</sub>, where M is the redox metal of the carrier or of the promoter). Thus, Rodriguez (30) reported that a chemical shift of +0.7 eV with respect to the metal would be expected if it is alloyed. In line with this and considering the XRD diffraction patterns of the used and reduced catalysts (Figs. 3c–e), it can be argued that a PdZn alloy is presumably formed upon H<sub>2</sub>-reduction at temperatures above 573 K. The observation of the Pd 3d<sub>5/2</sub> peak at 335.7 eV at reduction temperatures

of 373, 573, and 773 K for catalyst 1% Pd/ZnO (IW) and the shift from 335.2 eV at 573 K to 335.7 eV at 773 K for the parent catalyst 5% Pd/ZnO indicate that not only Pd loading but presumably Pd crystal size and metal–support interaction, among other factors, would be responsible for alloy formation.

The O 1s core level exhibited two components irrespective of Pd content and catalyst pretreatments. Catalyst 1% Pd/ZnO (IW) showed a major peak at a BE of 530.9–531.0 eV corresponding to lattice oxygen and a minor one at 532.7–533.0 eV assigned to surface hydroxyl groups. The relative proportion of these components changed with catalyst pretreatments (Tables 2 and 3). Thus, the intensity of the peak at ca 532.7 eV increased upon exposure to H<sub>2</sub> at room temperature and then decreased at higher reduction temperatures. This phenomenon can be explained on the basis of water adsorption/reaction at the ZnO interface and the further decomposition of the product at higher temperatures. The water generated in the course of PdO reduction ( $\text{PdO} + \text{H}_2 \rightleftharpoons \text{Pd} + \text{H}_2\text{O}$ ) is adsorbed on the ZnO surface where it is dissociated, leading to OH groups ( $\text{ZnOZn} + \text{H}_2\text{O} \rightleftharpoons 2\text{Zn-OH}$ ). While this last equilibrium may be shifted to the right side at lower temperatures, the decomposition of hydroxyl groups becomes a favored process at temperatures above 373 K.

Atomic Pd/Zn ratios have been also included in Tables 2 and 3. These ratios were calculated from peak area measurements and atomic sensitivity factors (24). For catalyst 1% Pd/ZnO the Pd/Zn XPS ratio is a maximum for the calcined and outgassed sample (0.047 and 0.045, respectively), but it decreases by about a 25% upon exposure to H<sub>2</sub> atmosphere at room temperature and even more (ca 34%) at 773 K. The dependence of the Pd/Zn ratio on pretreatments is somewhat different for the parent 5% Pd/ZnO catalyst. Upon H<sub>2</sub>-reduction at room temperature this ratio increases by a factor of about 3 with respect that of the calcined sample, and then it decreases drastically with increasing reduction temperature (58% decrease at 773 K). The decay of Pd/Zn XPS ratios upon reduction can be primarily associated to the well-known tendency of Pd to sinter. Moreover, if PdZn alloys are formed, the dilution effect of Zn in the alloy could explain the decrease of the Pd signal. As pointed out by Rodriguez (30), zinc tends to be segregated towards the surface of PdZn alloys. Therefore, one would expect that Zn-rich alloys or Zn segregation to the surface may occur upon increasing the reduction temperature. On the other hand, if alloy formation is favored at low temperatures, as is the case of 1% Pd/ZnO catalyst, no so-marked changes in the Pd/Zn ratio would be observed upon increasing the temperature of reduction.

#### Catalytic Activity

In order to explore the activity and selectivity behavior of Pd/ZnO catalysts, operation conditions under integral

regime and  $O_2/CH_3OH$  ratios in the feed close to the stoichiometry of Eq. [1] were selected. Preliminary runs were performed with catalyst 1% Pd/ZnO, using 0.5-g sample and flow rates ranging from 50 to 100 ml/min. As mass transport limitations were suggested to be involved in the oxidation reaction when working with the lowest flow rate, a feed rate of 100 ml/min was selected for activity tests. Two methanol compositions of 21.2 and 42.4% (molar) were explored as well. Due to the high exothermicity of the reaction, the occurrence of heat transport limitation may have increased the temperature of the catalyst particles significantly; thus, the real temperature is higher than that measured by the thermocouple inside the catalyst bed. In order to alleviate this uncertainty, the former composition (21.2% molar) was used in most experiments. It is emphasized at this point that a  $CH_3OH$  concentration in the feed stream of 21.2% is quite similar to that of a  $O_2/CH_3OH = 0.5$  which can be reached using air instead oxygen as an oxidant.

#### Catalyst 1% Pd/ZnO (IW)

Activity and product distributions in the methanol partial oxidation over catalyst 1% Pd/ZnO (0.5 g) at  $O_2/CH_3OH$  feed ratios of 0.3 and 0.5 are displayed in Figs. 7a and 7b, respectively. Within the temperature range 503–543 K, oxygen consumption was complete, while methanol conversions reached 40–80%. Hydrogen, water, carbon oxides, and unconverted methanol were the only products detected at the outlet of the reactor. Upon increasing the reaction temperature, methanol conversion increased with a simultaneous increase in  $H_2$  selectivity at the expense of water. Selectivity of  $CO_2$  also increased, although its increment was less marked (Fig. 7). Since  $O_2$  was completely consumed, this selectivity trend suggests some contribution of the methanol steam reforming produced by the water by-product. Furthermore, as illustrated in Table 4, the selectivities to the highest methanol conversions and fixed  $O_2/CH_3OH$  ratio can be predicted, considering that the additional methanol converted disappeared according to the steam reaction (Eq. [2]). Calculated data in Table 4 were obtained from experimental compositions at 503 K, using the stoichiometry of reaction [2] to predict the compositions to be attained if conversion increases up to the experimental value at 543 K. Table 4 also includes calculated values assuming  $CH_3OH$  decomposition (Eq. 3):



If the decomposition reaction (Eq. [3]) is involved, the calculated hydrogen proportion becomes much lower with, simultaneously, a much higher CO percentage than the experimental ones.

As illustrated in Fig. 8, the product distributions exhibited a marked dependence on the  $CH_3OH$  conversion. The data reported in Fig. 8, obtained by changing the reaction

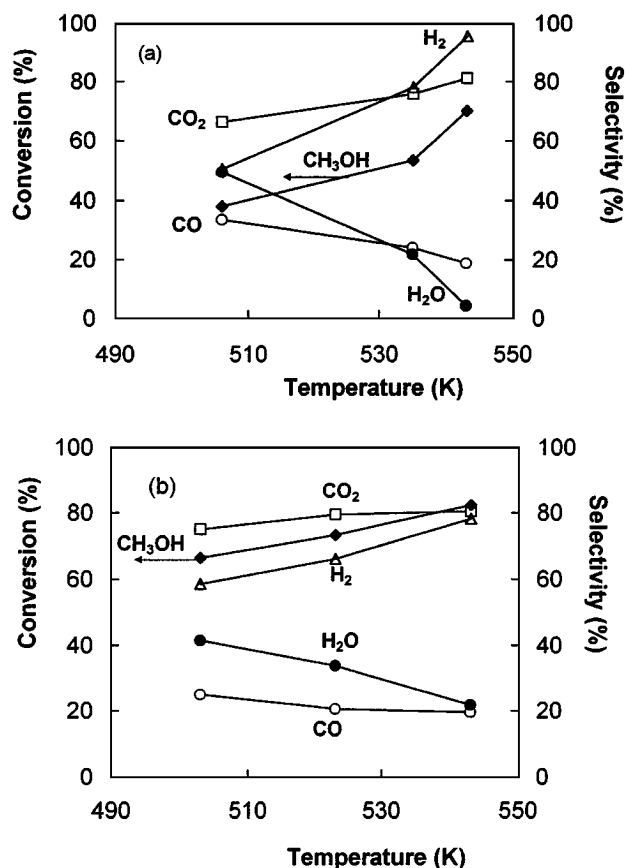


FIG. 7. Dependence of methanol conversion and selectivities on the temperature for the partial oxidation of methanol over catalyst 1% Pd/ZnO using feed ratios  $O_2/CH_3OH$  of 0.3 (a) and 0.5 (b).

temperature, revealed that very high  $H_2$  selectivities can be reached at high methanol conversions. This is clear for a ratio  $O_2/CH_3OH = 0.3$  in the feed, with which  $H_2$  selectivity of 96% can be attained at a  $CH_3OH$  conversion of 70%. Looking at the carbon oxide distribution,  $CO_2$  is dominant

TABLE 4  
Product Distributions in the Partial Oxidation of Methanol ( $O_2/CH_3OH = 0.3 M$ ) on Catalyst 1% Pd/ZnO Assuming the Contribution of Reactions [2] and [3]

	Experimental data <sup>a</sup>		Calculated data <sup>b</sup>	
	503 K	543 K	Eq. [2]	Eq. [3]
methanol conv (%)	38(66)	70(82)	70(82)	70(82)
carbon selectivity (%)				
CO	34(25)	19(20)	18(20)	64(39)
$CO_2$	66(75)	81(80)	82(80)	36(61)
hydrogen selectivity (%)				
$H_2$	50(58)	96(78)	96(76)	73(66)
$H_2O$	50(42)	4(22)	4(24)	27(34)

<sup>a</sup> Oxygen conversion = 100%.

<sup>b</sup> Starting from experimental data at 503 K. Data in parentheses are for  $O_2/CH_3OH = 0.5 M$ .

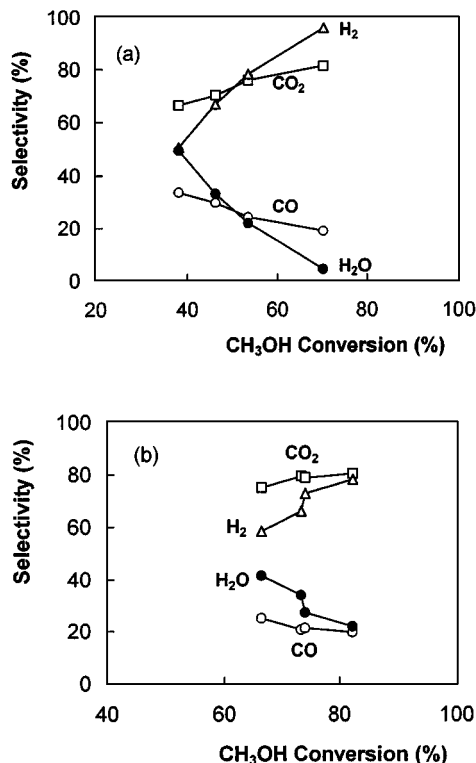
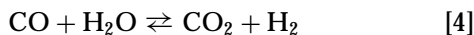
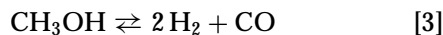


FIG. 8. Selectivities as a function of methanol conversion for the partial oxidation of methanol over catalyst 1% Pd/ZnO using feed ratios  $O_2/CH_3OH$  of 0.3 (a) and 0.5 (b).

although a certain proportion of CO is observed. From the data reported in Fig. 10 it becomes apparent that, upon increasing  $O_2$  in the feed stream, larger  $CH_3OH$  conversions are required to obtain the same  $H_2$  selectivity. The less-marked effect on carbon oxides points to a faster oxidation of  $H_2$  than CO.

The methanol steam reforming reaction (Eq. [2]) can be considered as a combination of the methanol decomposition (Eq. [3]) and water gas shift (WGS) reaction (Eq. [4]):



The  $H_2O$  (or the  $CO_2$ ) required for the WGS reaction comes from the deep oxidation of a fraction of methanol fed ( $CH_3OH + O_2 \rightleftharpoons H_2O + CO_2$ ). According to this reaction sequence, if the whole CO formed in the decomposition reaction (Eq. [3]) is consumed in the WGS reaction, coincidence in the proportion of products by steam reforming and by decomposition-WGS reactions could be expected. The scheme decomposition-WGS has been proposed by several authors (5,12,31) for the methanol steam reforming

over copper catalysts. On the other hand, Jiang *et al.* (32) and Takezawa *et al.* (15) excluded that reaction scheme and proposed a new one for the  $CH_3OH$  reforming, consisting in the reaction of oxygenate intermediates, such as formaldehyde or methyl formate with water vapor. These authors also argued that the WGS does not occur in the presence of methanol over copper catalysts. Furthermore, Takezawa *et al.* (15,16) proposed a reactional scheme based on the reforming of methyl formate or formaldehyde over Pd/ZnO catalysts. In our case, the observation of a certain proportion of CO and water among the reaction products indicate that the rate of WGS reaction is not fast. This finding also supports the hypothesis that the oxidation reaction might well occur through reforming of methanol or certain oxygenate intermediates, at least under the conditions used in the present study.

Figure 9 displays the changes in  $CH_3OH$  conversion produced upon catalyst exposure to the reaction mixture for long on-stream operation. At the two  $O_2/CH_3OH$  ratios (0.3 and 0.5), methanol conversion decreased around 8% for reaction times longer than 48 h. Moreover, selectivity does not change at a significant extent, as these data fit well with the whole set of data. It is worth noting that selectivity results from these life tests have been included in Fig. 8. The exothermicity of the reaction could be perceived by measuring the temperature at the catalyst bed and at the oven wall ( $T_{bed} - T_{wall}$ ). It can be seen in Fig. 9 that the slow deactivation observed in the catalyst subjected to on-stream operation for periods longer than 48 h is accompanied by a parallel increase of the  $T_{bed} - T_{wall}$ . While this difference amounts 9 K for a feed ratio  $O_2/CH_3OH = 0.3$  and reaction temperature of 503 K, it increases up to 28 K for a feed ratio  $O_2/CH_3OH = 0.5$  and reaction temperature of 543 K. If the reaction involves oxidation (exothermic) and reforming (endothermic) steps, higher heat evolution would be expected at lower rather than at the higher  $CH_3OH$  conversions.

#### Catalyst Weight and Dilution

With the aim to analyse the selectivity-conversion relationship an additional experiment was carried out using 0.20 g of catalyst 1% Pd/ZnO. However, conversion was similar to that using 0.50 g of catalyst (Fig. 10). There are no thermodynamic restrictions, although, as can be seen below, the strong exothermicity of the reaction could be responsible for this behavior. Figure 10 also shows the increase of  $CH_3OH$  conversion when increasing the  $O_2/CH_3OH$  ratio from 0.3 to 0.5. As this increase represents an increase in the oxygen partial pressure ( $P_{O_2}$ ) and a positive dependence order between  $P_{O_2}$  and reaction rate is expected, the observed trend is reasonable. As is well known, methanol conversion over Cu/ZnO catalysts is accelerated in the presence of oxygen (33–35). Although a similar mechanism could be involved in the oxidation of methanol over

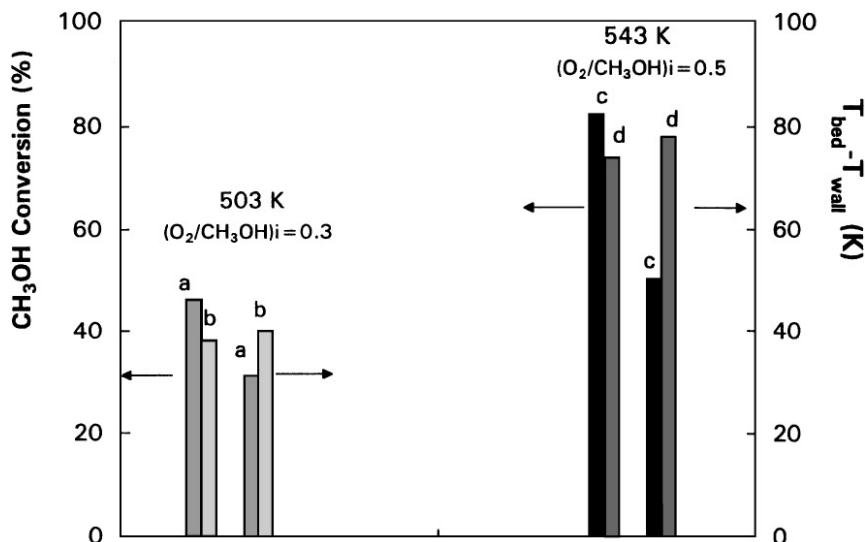


FIG. 9. Changes of the methanol conversion and  $T_{bed} - T_{wall}$  difference on the time on-stream for the partial oxidation of methanol over catalyst 1% Pd/ZnO: (a) 0–19 h; (b) 68–76 h; (c) 44–53 h; (d) 93–99 h.

Pd/ZnO catalysts; heat transport would influence the reaction when using higher  $P_{O_2}$  in the feed stream.

Upon catalyst dilution in SiC (SiC/Cat = 2/1), methanol and oxygen conversions decreased with respect to undiluted catalyst under the same experimental conditions (Fig. 10). This finding suggests that in the undiluted catalyst heat transport effects, presumably with hot spots within the catalyst bed, are involved in the oxidation reaction. Besides that, the heat transfer limitation can also cause significant radial temperature gradients which also influence the results. Catalyst dilution led to a less marked change in the methanol conversion upon increasing the temperature of reaction or  $O_2/CH_3OH$  ratio in the feed. Deactivation was also higher for the diluted bed (Fig. 12). One difference between the runs, with and without dilution, lies in the environment to which the catalyst was subjected. Since

methanol and oxygen conversions were lower in the diluted catalyst, the average partial pressure of the reactants over the catalyst surface was higher. The hypothesis of a faster deactivation of the catalyst in the presence of oxygen is not discarded. With respect to the convenience of operating under reaction conditions far from the isothermicity Jenkins and Shutt (36) pointed out that the use of a reactor, properly designed to operate with hot spots within the catalyst bed, could be appropriate to generate  $H_2$  from methanol according to Eq. [1]. Furthermore, in the comparison of isothermal and hot spot reactors these authors observed poorer performances in the conventional isothermal reactor.

The  $H_2$  selectivity during the partial oxidation of methanol over 1% Pd/ZnO catalyst for the three catalytic runs (0.5, 0.2, and 0.2 g with dilution in SiC) are displayed in Fig. 11.  $H_2$  selectivity was quite low at low  $CH_3OH$  conversions when  $O_2$  was not completely consumed, and it increased with increasing  $CH_3OH$  conversion. The converted  $O_2/CH_3OH$  ratio was higher than 1 at low conversions and approached the stoichiometric value of 0.5 (see Eq. [1]) with increasing conversion (Fig. 12).

In addition to the major products of the reaction ( $H_2$ ,  $H_2O$ ,  $CO_2$ , and  $CO$ ), a small proportion of  $HCHO$  was detected mainly at the lowest  $CH_3OH$  conversions. Therefore, the participation of the following reactions is envisaged to a certain extent when oxygen is present in the gas phase:

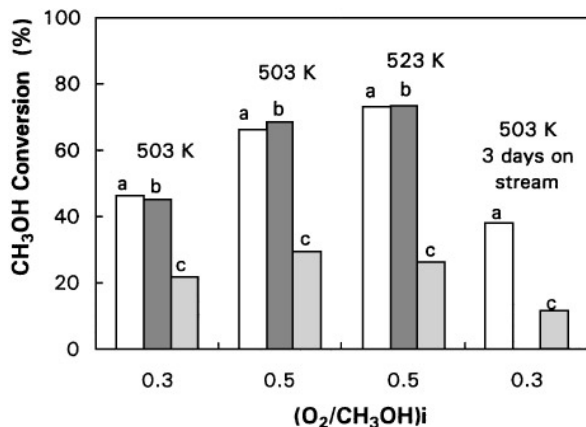


FIG. 10. Methanol conversion on catalyst 1% Pd/ZnO using different weights and SiC dilution: (a) 0.5 g; (b) 0.2 g; (c) 0.2 g + 0.4 g SiC.

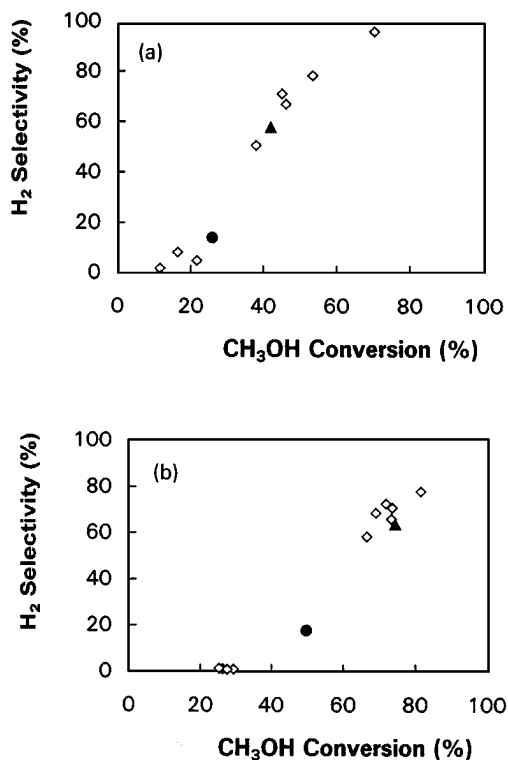


FIG. 11. Hydrogen selectivity over Pd/ZnO catalysts of different Pd loading for O<sub>2</sub>/CH<sub>3</sub>OH ratios of 0.3 (a) and 0.5 (b). (◇) 1% Pd; (△) 2% Pd; (●) 5% Pd.

The low H<sub>2</sub> selectivity observed at low methanol conversion may be due to the fast oxidation of hydrogen (Eq. [7]), produced by the other reactions (Eqs. [1], [2], [5], and [6]). On the other hand, as illustrated in Table 4, the contribution of the steam reforming reaction seems to be important when oxygen becomes completely consumed.

#### Palladium Loading

The dependence of methanol conversion at a reaction temperature of 503 K and feed ratio O<sub>2</sub>/CH<sub>3</sub>OH of 0.3 on

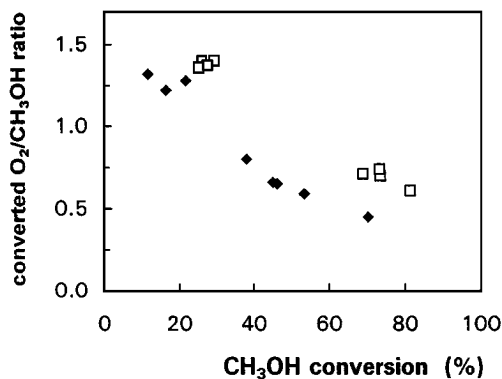


FIG. 12. Dependence of the consumed O<sub>2</sub>/CH<sub>3</sub>OH ratio on the methanol conversion over catalyst 1% Pd/ZnO for feed ratios O<sub>2</sub>/CH<sub>3</sub>OH of 0.3 (◆) and 0.5 (□).

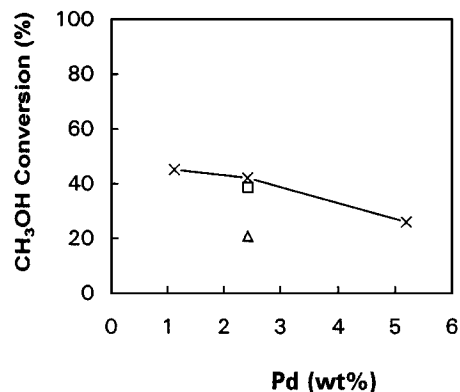


FIG. 13. Influence of the Pd content on the methanol conversion at 503 K and feed ratio O<sub>2</sub>/CH<sub>3</sub>OH of 0.3 and reduction temperatures of 473 K (□), 573 K (×), and 623 K (△).

the Pd/ZnO catalysts prereduced at 573 K are displayed in Fig. 13. The CH<sub>3</sub>OH conversion is essentially constant between 1 and 2% Pd and then drops slightly for catalyst 5% Pd/ZnO. With respect to product distribution some differences were observed among the catalysts. Catalysts 1% and 2% Pd/ZnO, which exhibited comparable conversion levels, displayed similar H<sub>2</sub> selectivity (Fig. 11). The exception of this tendency was catalyst 5% Pd/ZnO in which CO selectivity was enhanced with respect to the 1% and 2% Pd counterpart. In addition, HCHO selectivity over catalyst 5% Pd/ZnO was much higher. As a general tendency, H<sub>2</sub> (and CO) selectivity is directly related to CH<sub>3</sub>OH conversion; however, the behavior of catalyst 5% Pd/ZnO cannot be explained in terms of this trend. It is likely that processes such as methanol decomposition, inability to oxidize the intermediate HCHO, and low oxidation rate of CO might be involved in large PdZn alloy (and Pd) particles as that found on prereduced catalyst 5% Pd/ZnO.

#### Catalyst Pretreatments

There are literature reports which document the importance of the activation step on the performance of Pd/ZnO catalysts when used in the methanol steam reforming (15,16). It has been emphasized that catalyst activity is enhanced if PdZn alloy is allowed to be formed upon hydrogen pretreatment. In order to study the influence of H<sub>2</sub>-pretreatment on the performance for partial oxidation of methanol, catalyst 2% Pd/ZnO prereduced at three different temperatures was selected for this purpose. As already shown in Fig. 4, the selected temperatures of reduction of 473, 573, and 623 K represent different extents or levels of PdZn alloy formation. Therefore, this explored temperature range is expected to cover surface compositions from Pd-rich particles (473 K) to well-defined PdZn structures (623 K). Catalyst prereduced at 473 and 573 K yielded the same activity and decreased upon reduction at 623 K (Fig. 13). The selectivity of hydrogen followed a

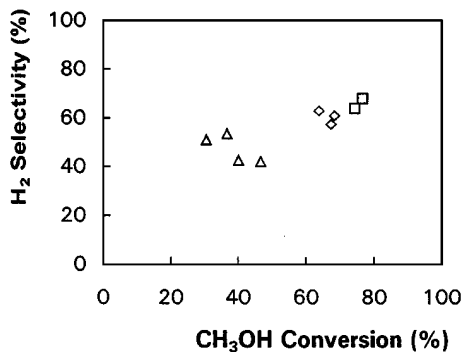


FIG. 14. H<sub>2</sub> selectivity (O<sub>2</sub>/CH<sub>3</sub>OH=0.5) for catalyst 2% Pd/ZnO subjected to different reduction temperatures: (◇) 473 K; (□) 573 K; (△) 623 K.

similar trend (Fig. 14), although the comparison of H<sub>2</sub> selectivity of this catalyst prereduced at 623 K with that of the parent 1% Pd/ZnO prereduced at 573 K (Fig. 11b) reveals a substantial improvement in the former. It appears that H<sub>2</sub> selectivity became enhanced in the catalysts in which PdZn alloy formation is favored. Even considering this beneficial effect, care must be taken to avoid high temperature pretreatments to minimize the sintering of metallic particles.

### CONCLUSION

ZnO-supported Pd catalysts are very active and selective toward hydrogen production in the partial oxidation of methanol. Catalyst performance has been investigated as a function of the Pd loading and pretreatment in hydrogen environment under feed ratios O<sub>2</sub>/CH<sub>3</sub>OH (molar) of 0.3 and 0.5 at 503–543 K. The dependences of the selectivities, the converted ratio O<sub>2</sub>/CH<sub>3</sub>OH, and, also, the evolved heat on methanol conversion were consistent with the reaction scheme: oxidation → reforming of methanol. As the oxidation reaction is exothermic and the operation was conducted, in general, using quite concentrated feed, important thermal effects were observed, with the undiluted catalyst bed showing a better performance than the diluted one. Catalyst characterization by TPR, X-ray diffraction, and XPS revealed that PdZn alloys can be formed upon reduction at moderate temperatures. A shift of +0.7 eV has been observed in the binding energy of Pd 3d<sub>5/2</sub> core level spectrum of the catalyst 5% Pd/ZnO prereduced at temperatures above 373 K, which agrees with that reported in the literature for alloyed palladium (16). Moreover, PdZn alloys appear to be formed even easily on catalyst 1% Pd/ZnO. This is confirmed not only by the observation of a component at 335.7 eV in the Pd 3d<sub>5/2</sub> core level at lower temperatures of reduction but also by the rather low surface-to-bulk Pd/Zn ratios in catalyst 1% Pd/ZnO compared to that of 5% Pd/ZnO. This is presumably a consequence of the stronger

metal–metal oxide interactions of the smaller Pd particles. The reactivity of the alloy seems to be somewhat different from that of Pd particles as for catalyst 5% Pd/ZnO the HCHO selectivity was much higher. The presence of PdZn alloys was also detected by X-ray diffraction on the 2% Pd/ZnO catalyst used on-stream. It is likely that processes such as methanol decomposition, inability to oxidize the intermediate HCHO and low oxidation rate of CO might be involved in large PdZn alloy particles since CO and HCHO selectivities were much higher for catalyst 5% Pd/ZnO. The reduction temperature appears as a critical parameter for the catalytic behavior. A compromise between enhancement in the H<sub>2</sub> selectivity and activity drop at increasing reduction temperatures was apparent.

### ACKNOWLEDGMENT

M.L.C. thanks the Central University of Venezuela and its CDCH Council for a sabbatical leave. Financial support from CICYT, Spain, under Projects MAT95-0894, JOE3-CT97-0049, and MAT96-2056CE is also acknowledged.

### REFERENCES

- Peña, M. A., Gomez, J. P., and Fierro, J. L. G., *Appl. Catal. A: General* **144**, 7 (1996).
- Jamal, Y., and Wyszynski, *Int. J. Hydrogen Energy* **19**, 557 (1994).
- Veziroglu, T. N., and Barbir, F., *Int. J. Hydrogen Energy* **17**, 391 (1992).
- Petterson, L., and Sjöström, K., *Int. J. Hydrogen Energy* **16**, 671 (1991).
- Amphlett, J. C., Creber, K. A., Davis, J. M., Mann, R. F., Peppley, B. A., and Stokes, D. M., *Int. J. Hydrogen Energy* **19**, 131 (1994).
- Kumar, R., Ahmed, S., and Yu, M., *Preprints, Am. Chem. Soc., Div. Fuel Chem.* **38**, 1471 (1993).
- Lindner, B., and Sjöström, K., *Fuel* **63**, 1485 (1984).
- Srinivasan, S., *J. Electrochem. Soc.* **136**, 41C (1989).
- Schmitz, A. D., Eyman, D. P., and Gloer, K., *Energy & Fuels* **8**, 729 (1994).
- Jiang, C. J., Trimm, D. L., and Wainwright, M. S., *Chem. Eng. Technol.* **18**, 1 (1995).
- Jiang, C. J., Trimm, D. L., Wainwright, M. S., and Cant, N. W., *Appl. Catal. A: General* **93**, 24 (1993).
- Huang, T. J., and Wang, S. W., *Appl. Catal.* **24**, 287 (1986).
- Huang, T. J., and Chren, S. L., *Appl. Catal.* **40**, 43 (1988).
- Alejo, L., Lago, R., Peña, M. A., and Fierro, J. L. G., *Appl. Catal. A: General* **162**, 281 (1997).
- Takezawa, N., and Iwasa, N., *Catal. Today* **36**, 45 (1997).
- Iwasa, N., Masuda, S., Ogawa, N., and Takezawa, N., *Appl. Catal. A: General* **125**, 145 (1995).
- Alejo, L., Peña, M. A., and Fierro, J. L. G., in "Proceedings of the 15th Iberoamerican Symposium on Catalysis, Cordoba, Argentina, 1996," Vol. 3, p. 1661.
- Lago, R., Alejo, L., Peña, M. A., and Fierro, J. L. G., *Stud. Surf. Sci. Catal.* **110**, 623 (1997).
- "The Merck Index. An Encyclopedia of Chemicals, Drugs and Biologicals," 12th ed. Merck, Rahway, NJ, 1996.
- Hong, Ch. T., Yeh, Ch. T., and Yu, F. H., *Appl. Catal.* **48**, 385 (1989).
- Sarkany, A., Zsoldos, Z., Furlong, B., Hightower, J. W., and Guzzi, L., *J. Catal.* **141**, 566 (1993).
- Zsoldos, Z., Sarkany, A., and Guzzi, L., *J. Catal.* **145**, 235 (1994).

23. Kim, K., Gossmann, A., and Winograd, N., *Anal. Chem.* **46**, 197 (1976).
24. Briggs, D., and Seah, M. P. (Eds.), "Practical Surface Analysis by Auger and X-Ray Photoelectron Spectroscopy. Wiley, Chichester, 1985.
25. Goetz, J., Volpe, M. A., Sica, A. M., Gigola, C. E., and Touroude, R., *J. Catal.* **153**, 86 (1995).
26. Hermann, P., Guigner, J. M., Tardy, B., Jugnet, Y., Simon, D., and Bertolini, J. C., *J. Catal.* **163**, 169 (1996).
27. Venezia, A. M., Rossi, A., Duca, D., Martorana, A., and Deganello, G., *Appl. Catal. A: General* **125**, 113 (1995).
28. Jones, M. G., and Nevell, T. G., *Appl. Catal.* **70**, 277 (1991).
29. Pitchon, V., Guenin, M., and Praliaud, H., *Appl. Catal.* **63**, 333 (1990).
30. Rodriguez, J. R., *J. Phys. Chem.* **98**, 5758 (1994).
31. Santacesaria, E., and Carra, S., *Appl. Catal.* **5**, 345 (1983).
32. Jiang, C. J., Trimm, D. A., Wainwright, M. S., and Cant, N. W., *Appl. Catal. A: General* **97**, 81 (1994).
33. Wachs, I. E., and Madix, R. J., *J. Catal.* **53**, 208 (1978).
34. Clarke, D. B., Lee, D. K., Sandoval, M. J., and Bell, A. T., *J. Catal.* **150**, 81 (1994).
35. Fu, S. S., and Somorjai, G. A., *J. Phys. Chem.* **96**, 4542 (1992).
36. Jenkins, J. W., and Shutt, E., *Plat. Met. Rev.* **33**, 118 (1989).